

# COMPARISON OF STRAINS AT THE SUPERSTRUCTURE OF A BRIDGE, OBTAINED WITH A MATHEMATICAL MODEL, WITH THOSE OBTAINED DURING FIELD TESTING USING FIBER OPTIC MONITORING EQUIPMENT

L. M. Arenas-García, R. Gómez-Martínez, A. D. García-Soto & J. A. Escobar  
Instituto de Ingeniería, UNAM, Mexico,  
[LarenasG@iingen.unam.mx](mailto:LarenasG@iingen.unam.mx), [RgomezM@iingen.unam.mx](mailto:RgomezM@iingen.unam.mx),  
[ADgarciaS@iingen.unam.mx](mailto:ADgarciaS@iingen.unam.mx), [jess@pumas.ii.unam.mx](mailto:jess@pumas.ii.unam.mx)

## ABSTRACT

Integration of tasks such as instrumentation, monitoring, calibration of mathematical models and experimental testing leads increasingly to develop intelligent structures with systems that allow quickly identification of misbehavior and practical details that will help organizing maintenance and repair works, as well as prevent damage or catastrophic failures. Because bridge safety is an important issue in road management, structural health monitoring (SHM) has become a very useful tool for the management of these structures. This paper describes an implemented monitoring system in the Chiapas Bridge developed to study its structural behavior. Also, a series of load set ups and results of these tests are described and compared with results obtained from a simplified mathematical model. Study of strains induced by temperature changes and strain records obtained on site due to passing trucks is described as well.

## 1. INTRODUCTION

Experimental load tests, using instrumentation, have been widely used to assess performance and structural capacity of bridges, as well as to evaluate the condition of damaged bridges or even to determine the efficiency of repairs. Field tests are also useful to more accurately evaluate the ability of a bridge to distribute live loads [1]. Field inspection and periodic evaluation are needed for early detection of damage and to determine the safety and reliability in a consistent and up-to-date approach [2].

Regarding instrumentation, because of advances in the developing of new sensors, one of the main objectives of this work is to check the effectiveness of optical fiber sensors, which may also be used in practical conditions for the registration of deformation during load testing. Another of the main objectives of this work is to develop a mathematical model of the Chiapas Bridge reproducing properly its responses due to the passage of vehicles. With a calibrated model it would be possible to predict causes affecting the bridge with a better approximation than with a model based on design codes, since in many occasions the latter tend to underestimate the structural response [3].

Finally, it is shown how a system of continuous monitoring, using optical fiber sensors, can provide quantitative information about the response of a bridge under live loads and environmental changes, and a rapid prediction of the integrity of the structure. Also, it is shown how to use an initial database of the structure, in good condition, for the assessment and management of the future status of the bridge.

## **2. THE STRUCTURE AND ITS INSTRUMENTATION**

The bridge is located in the State of Chiapas, is part of the road segment between Las Choapas, Raudales Malpaso and Ocozocoautla de Espinoza; it is located in kilometer 961+731. The bridge has a total length of 1,208 m with eight spans: one of 124 m, five of 168 m, one of 152 m and one of 92 m. Width of its carriageway is 10m to provide enough room for 2 traffic lanes. Its maximum height is about 80 m from the bottom of the reservoir. As any other bridge, it is composed of three main parts: foundation, substructure and superstructure. This article only examines the superstructure which consists of 102 (segments) dowels of structural steel A-50. These were built in an assembly ditch collinear to the axis of the bridge forming trains of segments in the necessary amount to save each span of the bridge during launching [4].

The bridge was put into operation since 2003, but it was not until 2008 that was instrumented with optical fiber sensors placed along the structure [5]. In spite of receivers and transmitters being more expensive, humidity of the region and extreme changes in temperature provided the reasons to select optical fiber sensors. These are low weight, small size and resistant; uniform operation from -55°C to +125°C without degradation of their characteristics; and water and corrosion resistant with with adequate protection [6].

Because different fiber optic sensors can be combined in the same fiber, two types of sensors were used in the bridge: strain and temperature, and placed in certain cross segments at certain distances and were located so that they facilitate identification and measurements of variables. To organize monitoring, two arrays of sensors were designed for different segments of the bridge. In some arrays (type A), only four strain sensors were placed, and in other arrays (type B), in addition of these four sensors, two more temperature sensors were installed (Figure 1). Sensors were placed on the bottom plate as well as on the top plate inside the superstructure. A total of 82 sensors were installed along the bridge; 64 are used to monitor strains and 18 to monitor temperature. All of them were grouped into 16 segments defining a specific recording channel for each segment. Furthermore, in spans 4 and 8, cross segments located at  $\frac{3}{4}$  y  $\frac{1}{4}$  of the span length were also instrumented. Electric power is supplied by means of a photovoltaic system.

### 3. MONITORING OF STRAINS IN THE SUPERSTRUCTURE

Only strains due to temperature changes and truck loads are discussed herein. To determine the effects of temperature increments on the bridge, time history records of the monitoring are compared. And to determine the effects of passing loads on the bridge, tests were conducted using relatively heavy trucks. In addition, a mathematical model was developed to reproduce the effects due to these loads. These two approaches for monitoring and their results are presented in the following paragraphs, and a comparison of analytical data with results of field tests as well.

The monitoring system contained special software [7] that was used for processing the information recorded during the total length of the experimental program.

#### 3.1 Monitoring of strain increments due to temperature

To assess the effects of temperature gradients, it was necessary to revise cycles of increments throughout the day, for several days, and see how strains are developed in the different segments along the bridge. Temperature records for structural analysis obtained in the bridge were recorded at a frequency of 0.067 Hz, i.e. every 15 s. Because temperature magnitude depends on sunlight and temperature varies gradually during the day, shorter intervals were not considered because records would be very large and difficult to process. Besides, it would demand more energy from the photovoltaic system.

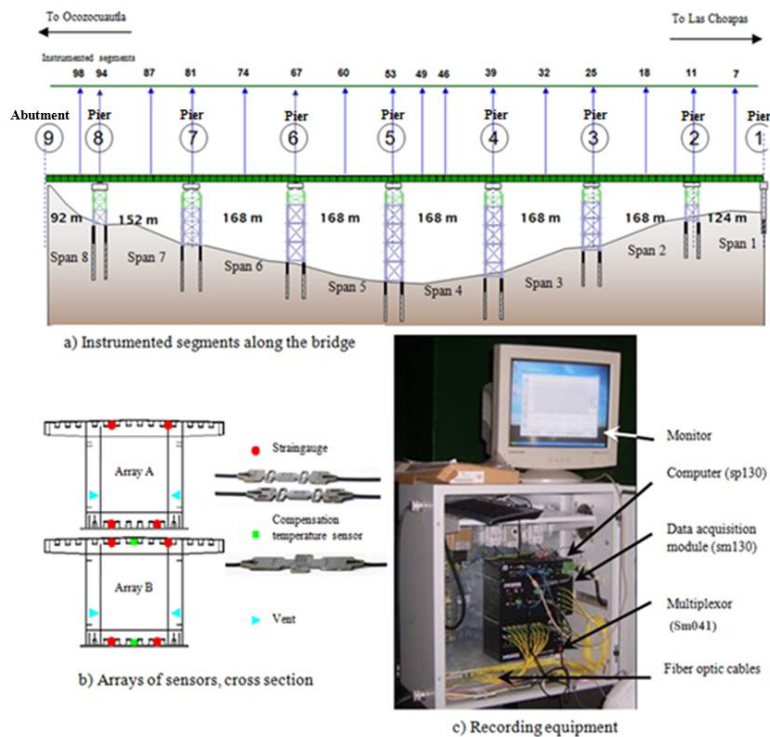
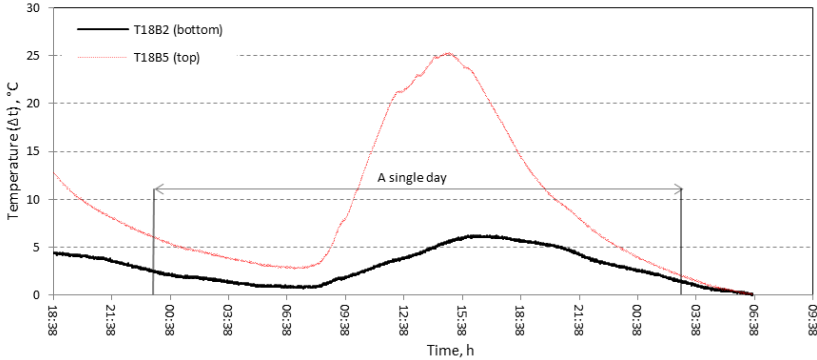


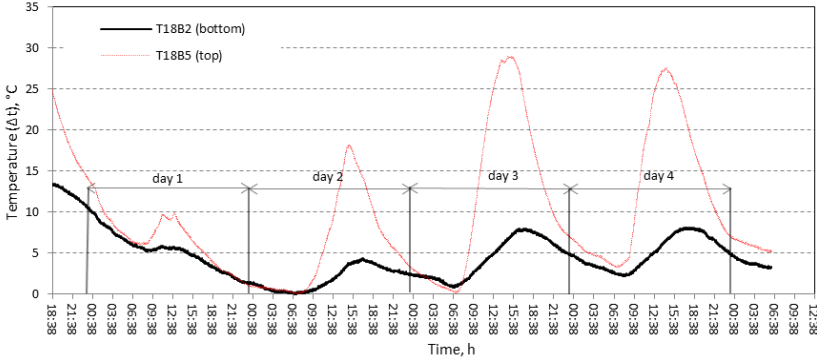
Figure 1 - Instrumentation with fiber optic sensors

In this paper we only present two temperature records. The first one was named EsC31 and contains data along a day and a half; the second one, E15sC44, contains data corresponding to four and a half days of continuous monitoring. Figure 2 shows these temperature records, normalized with respect to the minimum temperature, recorded in a segment at the center of a 168 m span (between piers 2 and 3, specifically). T18B2 denotes the sensor located at the bottom plate and T18B5 is related to the sensor on the top plate.



Maximum for T18B2	6.237474 $\mu\text{m/m}$	Maximum for T18B5	25.316747 $\mu\text{m/m}$
Minimum for T18B2	0	Minimum for T18B5	0

2a. Test EsC31, temperature increments at segment 18, span of 168 m



Maximum for T18B2	13.488962 $\mu\text{m/m}$	Maximum for T18B5	29.005779 $\mu\text{m/m}$
Minimum for T18B2	0	Minimum for T18B5	0

2b. Test E15sC44, temperature increments at segment 18, span of 168 m

Figure 2 – Temperature strain increments at the central cross segment of a 168 m span

At certain hours of the day, it was observed a large change in temperature and therefore in the deformation. E15sC44 test was the most representative on the third day of monitoring. The most part of the increase in temperature practically occurs between 9:00 AM and 3:00 PM, from the lowest recorded to the highest

during the day. Regarding the increment in  $\mu\text{m/m}$ , this exceeds  $270 \mu\text{m/m}$ . From 11:05 AM to 11:16 AM, a variation of  $1^\circ\text{C}$  produced up to  $15 \mu\text{m/m}$ .

### 3.2 Monitoring of strain increments due to vehicle loads (field tests)

Load tests were aimed to follow-up and obtain records of strain increments produced on the superstructure due to permit trucks [7], passing on the bridge. Once obtained, these increases were compared with those calculated using a simple analytical model with the intention of reviewing and improving maintenance and task inspections of the bridge. This, of course, depends on the accuracy of the calibration of the analytical model.

Vehicle load (dynamic) tests in the Chiapas Bridge took place in June 2010 using 2 trucks: a T3-S2 with gross weight of  $158279.331 \text{ N}$ , and a T3-S3 with gross weight of  $271742.2715 \text{ N}$  (Table 1).

Table 1- Characteristics of trucks used for the tests

Truck	Axis	Weight per axle (N)	Distance between axles (m)
T3-S2	1	4.61	0
	2	3.64	4.6
	3	3.12	1.5
	4	2.47	10.56
	5	2.3	1.3
T3-S3	1	4.02	0
	2	6.61	4.4
	3	6.94	1.35
	4	5.64	7.1
	5	3.3	1.2
	6	3.2	1.2

Only results of four out of a total of twelve tests will be presented herein. They are:

- 1) Test 1.- Truck T3-S2 running on one lane, direction Ocozocoautla-Malpasó, average speed:  $6.5 \text{ km/h}$ .
- 2) Test 3.- Trucks T3-S2 and T3-S3 running in parallel, one on each lane, direction Ocozocoautla-Malpasó, average speed:  $54.6 \text{ km/h}$ .
- 3) Test 5.- Trucks T3-S2 and T3-S3 running in opposite directions (round trip), average speed:  $59.7$  and  $57.3 \text{ km/h}$ , respectively.
- 4) Test 11.- Trucks T3-S3 and T3-S2 running in parallel, direction Tuxtla – Malpasó, average speed:  $53.9 \text{ km/h}$ .

To avoid interference in the capture of strain/deformation records, due to other vehicles, traffic was interrupted during the testing, before and after the trucks crossed the bridge. Data were recorded with a maximum of  $125 \text{ Hz}$  sampling rate i.e. a sample every  $0.008 \text{ s}$ . Thereby, records showed sufficient resolution despite the velocity of trucks, which was relatively high. This fact allowed a reduction in the time of halting the traffic in each lane.

Figure 3 shows an example of data with and without filtering, of test 1 in segment 18 of the bridge (Figure 1). Using the MATLAB program [9], these data were filtered by means of a low pass filter of 1 Hz as the maximum frequency. The filtering facilitates estimation of  $\mu\text{m}/\text{m}$  increments. Regarding the nomenclature used in the figures, S represents a strain-gauge and T a temperature sensor. Both literals are followed by the number of segment where the sensor is located. A and B are used to identify the array of sensors (see Figure 1), and the last number defines the position of each sensor in the cross-section of each segment, for array A: 1 = bottom left, 2 = bottom right, 3 = top left, 4 = top right; for array B: 1 = bottom left, 2 = bottom center, 3 = bottom right, 4 = top left, 5 = top center and 6= top right.

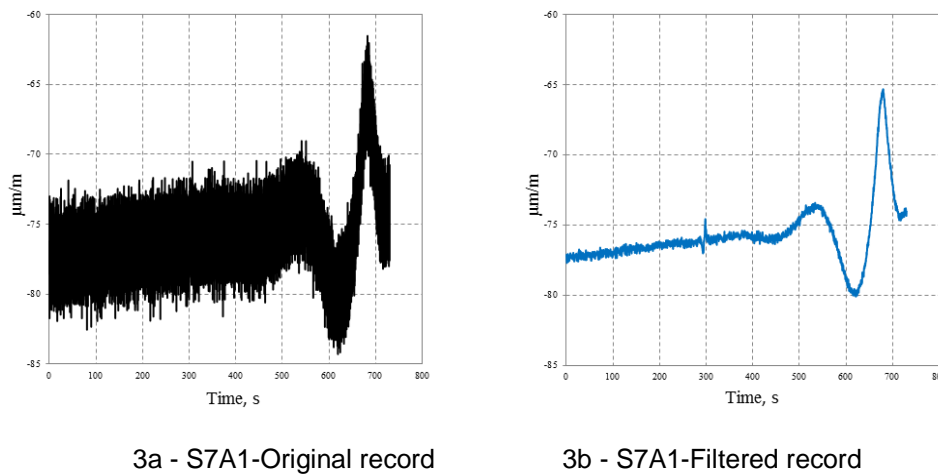
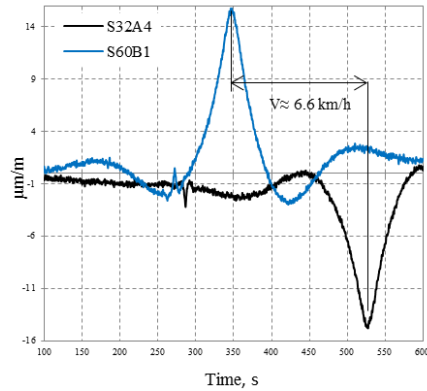
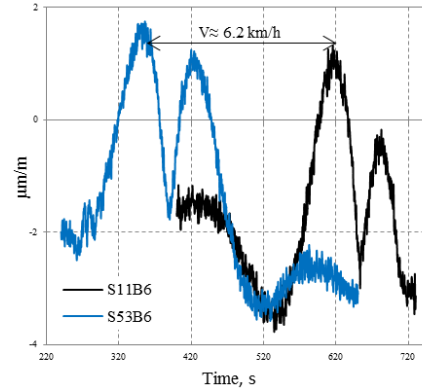


Figure 3 – Results of test 1

Analysis of stresses increments produced during the tests was performed with the filtered data. Figure 4 presents deformations increments caused by the passage of the T3-S2 truck in two different spans of 168 m. Sensor S32A4 was installed on the top plate of segment 32, whereas sensor S60B1 was located at the bottom plate of the box cross-section of segment 60 of the bridge. It is shown that in both cases the value of the increase is almost the same ( $15 \mu\text{m}/\text{m}$ ) but in opposite directions, one in tension and the other in compression. Figure 4b shows the increase of deformation in two sensors located at piers 2 and 5, respectively, both for test 1. Due to the time it takes for the truck to pass an instrumented segment to another one, an out of phase detail is observed in this Figure. Knowing that the distance from sensor S32A4 to S60B1 is 336 m, and from S11B6 (segment 11) to S53B6 (segment 60) is 504 m, is possible to estimate an average speed of the truck, 6.4 km/h.



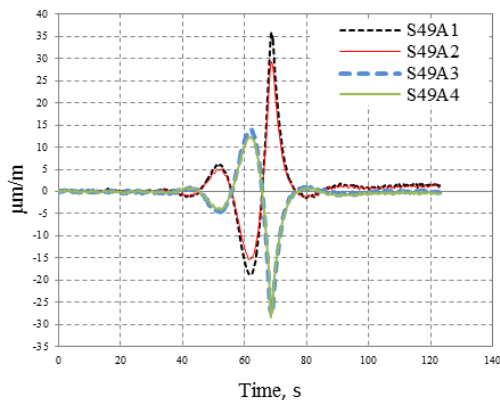
4a Sensors S32A4 and S60B1



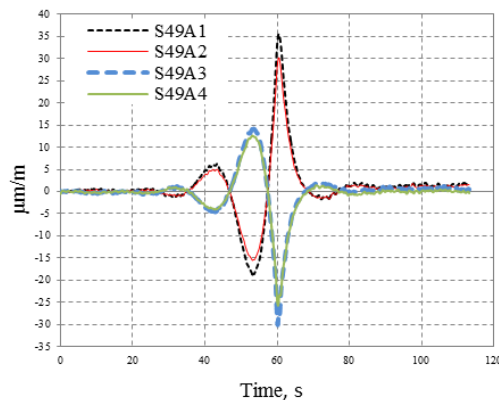
4b Sensors S11B6 and S53B6

Figure 4 – Time histories of strains, test 1

Figure 5 shows evidence of experimental results recorded at the four sensors in segment 49 during tests 3 and 11, which have similar conditions in terms of speed and direction. In this comparison, for all segment, it was observed that passing the truck on either lane does not represent any influence, because strains are very similar, and the effect is similar to a point load passing on the bridge, as well.



5a Test 3, at  $\frac{3}{4}$  of a 168 m span



5b Test 11, at  $\frac{3}{4}$  of a 168 m span

Figure 5 – Comparison of strain increments, tests 3 and 11

#### 4. ANALYTICAL MODEL

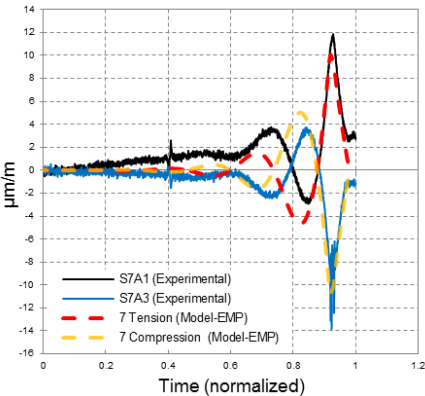
The analytical model was developed with the program SAP2000 [9, 10] using beam elements, which formed a continuous beam of 8 different cross segmentes. Analyses were used to reproduce the results of field tests in the time domain, defining vehicles and their speeds during each test. Hooke's law was used to compare experimental and analytical micro-deformations and stresses.

Step by step analyses were used to simulate experimental tests. These analyses in turn were divided into two types depending on the assignment of loads: load static multi-step (EMP) and time response (RT). Analyses were linear and only loads by axis and the transverse distribution of these were considered.

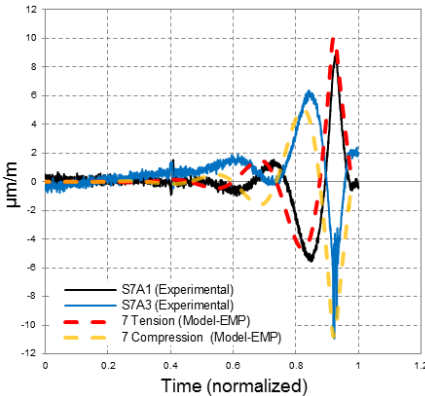
For the type of static load multi-step analysis, it was assumed that the speed of vehicles have no effect on the results, except the knowledge in change of position between one and another load to pass over the bridge; for this type of analyses dynamic effects are important and different results can be expected depending on the speed of vehicles.

Figure 6 shows the experimental deformations at segment 7 in a 124 m span, recorded at sensors on the top (S7A1) and at the bottom (S7A3) during experimental test 1. Also, the time history deformation obtained with the analytical model using the step by step analyses (EMP and RT) are shown. For plotting the results, because the difference of steps for the time histories, both responses (analytical and experimental) were normalized with respect to the total duration of each test. Because only 6 instrumented segments of the bridge had temperature sensors and trying to have more coherent results, a correction was made taking into account the proximity of segments with and without these sensors. No big differences were observed after this correction.

Differences between the maximum tension and compression strains of the experimental static test with the multistep dynamic analysis (EMP, plots 6a and 6b) are 1.82 and 3.05  $\mu\text{m}/\text{m}$ , respectively, being higher the experimental. On the other hand, differences of the maximum experimental results with the time response analysis (RT, plots 6c and 6d) were 1.79  $\mu\text{m}/\text{m}$  in tension, and 3.05  $\mu\text{m}/\text{m}$  in compression; again the experimental are little higher. Finally, the differences between the EMP and the RT analyses, in tension and compression, were of 03  $\mu\text{m}/\text{m}$  being EMP slightly higher than analysis RT. It is worth to mention that test 1 is quasi-static.

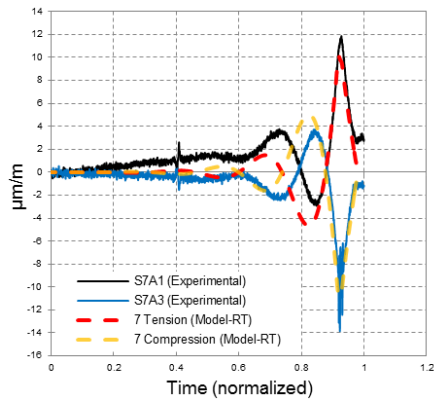


6a - without temperature correction

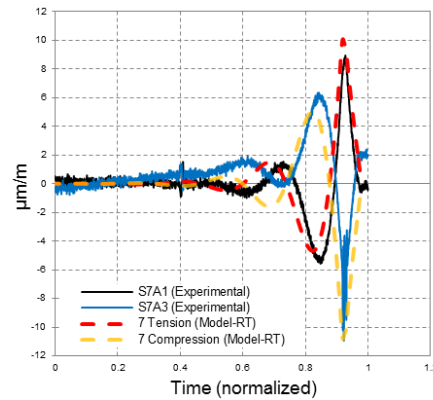


6b - with temperature correction





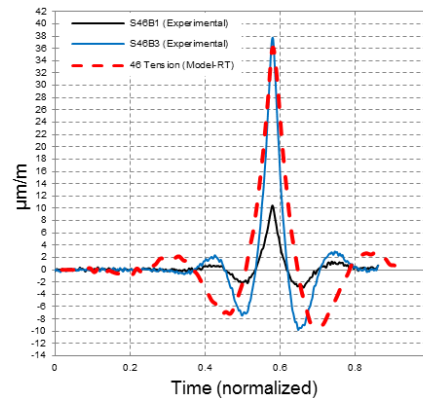
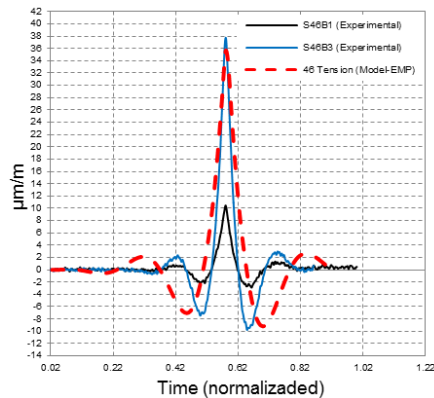
6c - without temperature correction



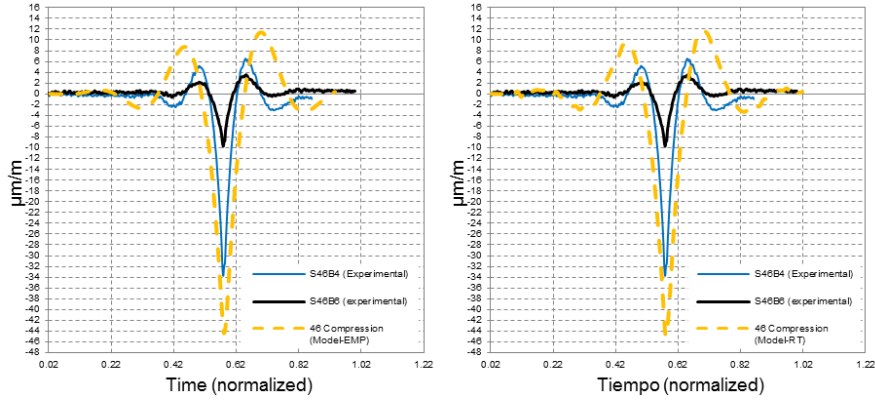
6d - with temperature correction

Figure 6 - Comparison of theoretical and experimental micro-strains increments, test 1

A comparison of analytical data with experimental results obtained during test 3, for segment 49 in a span of 168 m, is presented in Figure 7. The greater increases in deformation were attained in this test. It is observed that analytical and experimental tension strains are very similar between them, being slightly larger the latter, whereas compression strain differences are 11  $\mu\text{m}/\text{m}$  with respect to EMP and 11.2  $\mu\text{m}/\text{m}$  to RT. It is observed in these graphs that sensors S46B1 and S46B6 might be producing erroneous data, because of their lower magnitude of strains.



7a - experimental vs step by step analysis EMP and RT, 168 m span, bottom of the bridge (tension).



7b - experimental vs step by step analysis EMP and RT, 168 m span, top of the bridge (compression).

Figure 7 – Comparison of analytical and experimental deformations, test 3

Figure 8 shows results of test 11; features are similar to those of test number 3 and that regarding tension forces, there are no differences of the micro-strains magnitudes between these tests; compression strains differs very little, only 2  $\mu\text{m/m}$ .

For the whole bridge and for some tests, information was recorded along the total duration of the test. Below is a series of graphs of test 5 corresponding to various stages of passage of trucks over the bridge: approaching or moving forward each other in different lanes in the same span, crossing and departing or going away from the same span (see Figure 9). Again, experimental deformations are compared to strains obtained with the mathematical model, although only results from a sensor in compression are shown and the comparison with the step by step analysis of the time response (RT). On the middle part of the figure there are also illustrations of the simulations produced with the mathematical model. Differences, about 5  $\mu\text{m/m}$ , between analytical and experimental tests are shown along the way. In most cases the results of RT analysis are greater than the experimental ones.

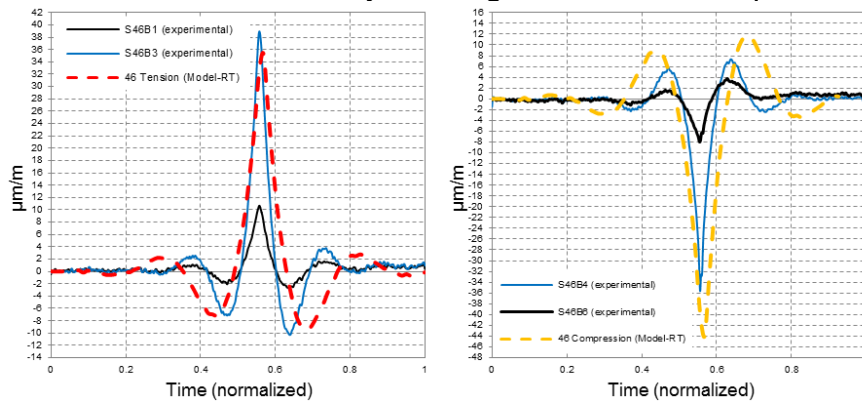
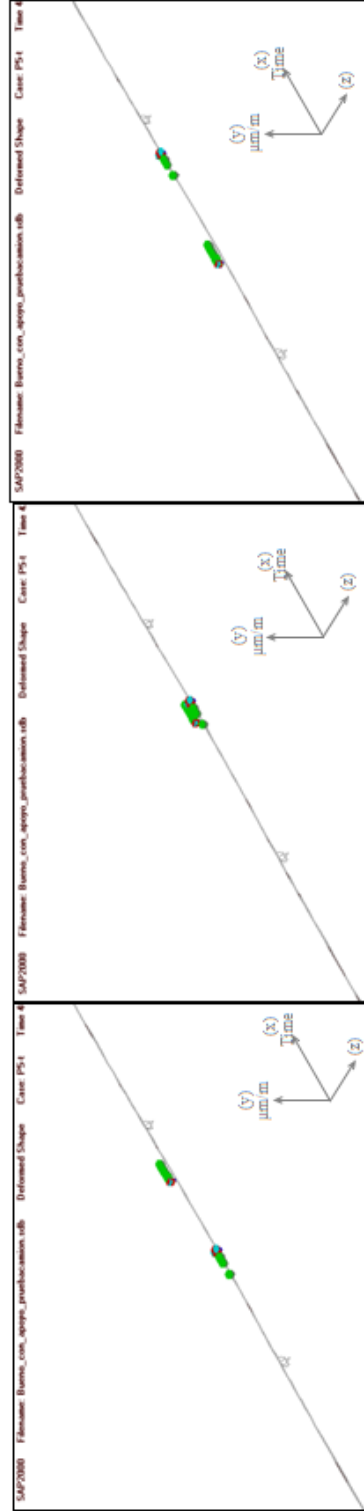
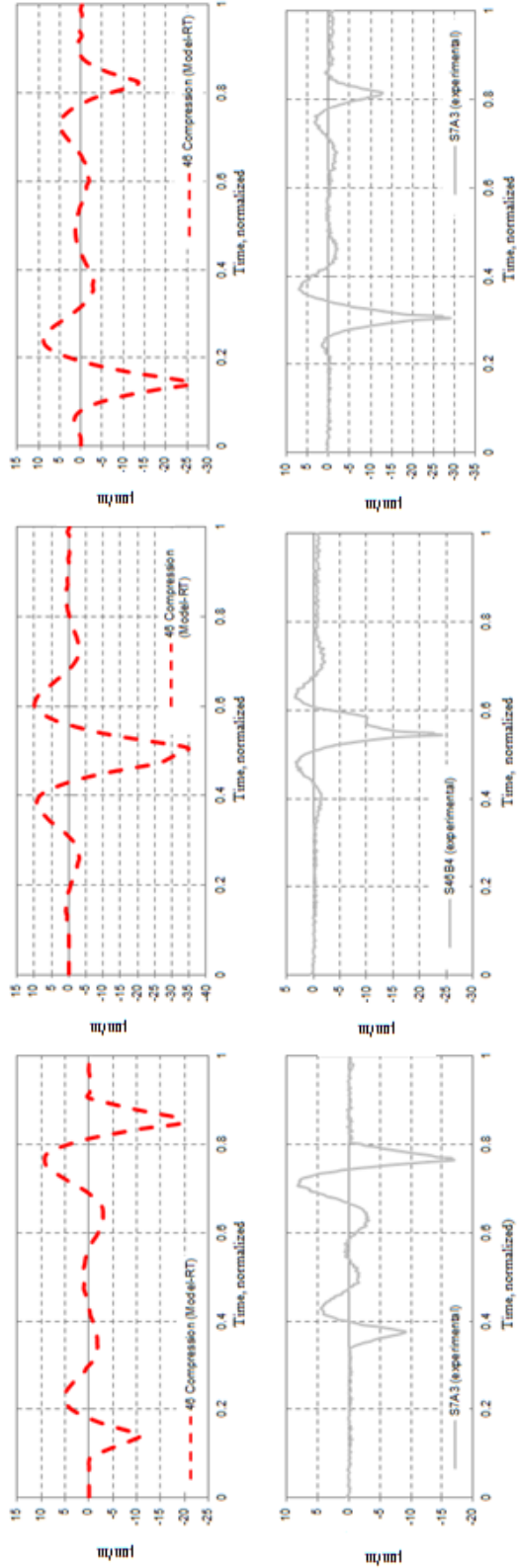


Figure 8 – Comparison of analytical and experimental deformations, test 11



trucks approaching

trucks crossing

trucks going away

Figure 9 – Different stages of trucks running on the bridge, analytical and experimental responses

## **5. FINAL COMMENTS**

Based on the results obtained it is concluded that the model reproduced, in an acceptable manner, experimental responses recorded during testing. The maximum difference of deformation between the model and the experimental results of the tests was about 17%.

The mathematical model took into account several factors in the response of the bridge. This can be adequately represented when considering thermal effects. It is possible that variations observed in the response of some elements, between the experimental data and the computer model response could be caused by uncertainties in the effects of thermal expansion.

It was noted that thermal effects produce more significant quantities of deformations compared to those produced by live loads or vehicles used in the field tests, with a maximum difference of 85%.

The largest increases in  $\mu\text{m}/\text{m}$  produced by truck loads were found in tests 3 and 11, specifically in segments 60 and 74, which suggest the existence of areas of concentration of stresses. Slight better results are obtained with the multi step by step analysis (RT) than with the time response analysis (EMP).

Although the instrumentation of the bridge with strain and temperature sensors sheds much valuable information that helps to understand aspects of the behavior of the bridge, is advisable to reinforce the monitoring of the structure with the implementation of other instruments, including a certain level of redundancy to have better control.

## **6. ACKNOWLEDGMENTS**

To David Muriá-Vila for his advise during the initial stages of monitoring. To Adrian Pozos, Miguel A. Mendoza, Raúl Sánchez, Oscar Rosales, Omar Rosales, Daniel Aldama and Pablo Arenas for their support to carry out this work. The first author acknowledges the financial support provided by the Institute of Engineering of the National Autonomous University of Mexico.

## REFERENCES

1. Hirachan, J. (2006). Development of Experimental Influence Lines for Bridges. Master thesis. Delaware University. Newark, EEUU.
2. I-Wen Wu, Chung-Yue Wang, Ming-Hung Chen, Hao-Lin Wang, Allen Cheng, Patrick Tsaia, David Wu, Hung-Wei Chang Chien and Hentai Shang (2007). Fundamental Problems of Optoelectronics and Microelectronics III. Edited by Kulchin, Yuri N.; Ou, Jinping; Vitrik, Oleg B.; Zhou, Zhi. Proceedings of the SPIE, Volume 6595, pp. 65952Y.
3. Andersson A., Karoumi R. and Sundquist H. (2006). Static and dynamic load testing of the new Svinesund Arch Bridge”, International Conference on Bridge Engineering-Challenges in the 21<sup>st</sup> Century, Hong Kong, China.
4. Gómez, R., Murià Vila D., Sánchez R., Escobar J.A., Muñoz D., and Vera R., (2004). Construction of the Chiapas bridge superstructure, Mexico. International Symposium on Steel Bridges, Millau France, pp 23-25.
5. Gómez, R., Murià, D., Mendoza, M., Méndez A., Chandler K., Sánchez R., Escobar J.A., and Csipkes A., (2009). Novel structural monitoring system for the Chiapas bridge. 4th International Conference on Structural Health Monitoring on Intelligent Infrastructure, July Zurich, Switzerland.
6. Micron Optics Inc. (2005). Optical Fiber Sensor Guide: Fundamentals and Applications. Manual. Atlanta, GA, USA.
7. Micron Optics Inc. (2008). Sensing Analysis Software ENLIGHTPro. User Guide, revision E. Atlanta, GA, USA.
8. SCT (2008). NOM-012-SCT-2-2008. Diario Oficial de la Federación, November, Mexico.
9. Matlab 7.7.0471 Release 2008b, MathWorks, Inc.
10. SAP2000 (2009). Sap2000 Advanced 14.1.0, 2009. Computers and Structures, Inc.
11. SAP2000, Version 12, User’s Manuals, Computers and Structures, Inc., Berkeley, California, 008, 474 pages.